Bioorganic & Medicinal Chemistry 20 (2012) 5296–5304

Contents lists available at SciVerse ScienceDirect

Bioorganic & Medicinal Chemistry

journal homepage: www.elsevier.com/locate/bmc

New hypotheses for the binding mode of 4- and 7-substituted indazoles in the active site of neuronal nitric oxide synthase

Elodie Lohou [a], Jana Sopkova-de Oliveira Santos [a], Pascale Schumann-Bard [b], Michel Boulouard [b], Silvia Stiebing [a], Sylvain Rault [a], Valérie Collot [a,*]

[a] Université de Caen Basse-Normandie, EA-4258 CERMN, FR CNRS 3038 INC3M, SF 4206 ICORE, UFR des Sciences Pharmaceutiques, Boulevard Becquerel, F-14032 Caen, France
[b] Université de Caen Basse-Normandie, EA-4259 GMPC, UFR des Sciences Pharmaceutiques, Campus 5 'Santé', Jules Horowitz, Boulevard Becquerel, F-14032 Caen, France

ARTICLE INFO

Article history:
Received 29 March 2012
Revised 11 June 2012
Accepted 13 June 2012
Available online 3 July 2012

Keywords:
Neuronal nitric oxide synthase inhibitors
7-Nitroindazole
4-Substituted indazoles
N-Alkylation
Microwave-promoted palladium-catalysed cyanation
Binding mode in the nNOS active site

ABSTRACT

Taking into account the potency of 4- and 7-nitro and haloindazoles as nNOS inhibitors previously reported in the literature by our team, a multidisciplinary study, described in this article, has recently been carried out to elucidate their binding mode in the enzyme active site. Firstly, nitrogenous fastening points on the indazole building block have been investigated referring to molecular modeling hypotheses and thanks to the in vitro biological evaluation of N_1- and N_2-methyl and ethyl-4-substituted indazoles on nNOS. Secondly, we attempted to confirm the importance of the substitution in position 4 or 7 by a hydrogen bond acceptor group thanks to the synthesis and the in vitro biological evaluation of a new analogous 4-substituted derivative, the 4-cyanoindazole. Finally, by opposition to previous hypotheses describing NH function in position 1 of the indazole as a key fastening point, the present work speaks in favour of a crucial role of nitrogen in position 2.

1. Introduction

Over the last decades, nitric oxide (NO) has grown on as an original biological messenger because of its free radical and gaseous nature[1] as well as its specific mode of action. This molecule is produced essentially in neurons, endothelial cells and macrophages during the conversion of L-arginine to L-citrulline catalyzed by three major isoforms of NO Synthases (NOS). The neuronal and endothelial enzymes (nNOS and eNOS) are constitutive and Ca^{2+}-dependent, whereas the inducible one (iNOS) is Ca^{2+}-independent and mostly expressed in activated macrophages.[2,3] Nevertheless, both enzymes appear as heme homodimers through which an electron flux can circulate between a reductase domain and an oxygenase one. The redox reaction series needs the presence of six cofactors: NADPH, FAD, FMN, tetrahydrobiopterin, calmodulin and calcium.[3–5] As a gas NO easily diffuses until neighbouring target cells and can interact with various proteins thanks to a direct or an indirect mechanism.[3,6] In the first case, it bonds to the heme enzyme iron atom to modulate the biological activity (activation of soluble guanylate cyclase or retroinhibition of NOS…). In the second case, it can also react with other free radicals to lead to specific molecular modifications like reversible S-nitrosylations[7] (activation of tissue plasminogen activator…).

NO is implicated in a wide range of physiological processes, including regulation of vascular tone and cerebral blood flow[8] as well as control of platelet aggregation.[5] Indeed, it activates from endothelial cells the soluble guanylate cyclase in smooth muscle cells and platelets which induces calcium concentration decrease.[3,4] Moreover, NO is involved in glutamatergic neurotransmission since NMDA receptor stimulation provokes nNOS activation, but it can also act as a direct messenger in the nervous nitridergic system.[3,9] As such, it intervenes in pain perception[10–12] and memorization.[12,13] Finally, NO takes part in fight against invading pathogens after a massive release by iNOS and thanks to its cytotoxic free radical properties.[3]

However, overproduction of NO, especially by nNOS and iNOS, plays a role in several disorders such as post-ischemic stroke damage[14–16] and neurodegenerative diseases.[17,18] Indeed, it exacerbates oxidative stress and glutamatergic excitotoxicity. Moreover, it is also involved in migraine headaches[2,19] and sustained hypotension during septic shock[20] since it provokes a massive vasodilatation. Thus, it is crucial to develop new selective nNOS inhibitors with potential antinociceptive properties and neuroprotective functions during ischemia or in case of Alzheimer's disease, but which would not perturb eNOS and its beneficial vascular effects. Despite a quite low homology between the three human NOS primary sequences (approximately 50%), the overall folds and the active site are very closed in the three NOS oxygenase domains (NOSox). With this in mind, specific inhibition of one isoenzyme constitutes a significant

* Corresponding author. Tel.: +33 2 31566815; fax: +33 2 31566803.
E-mail address: valerie.collot@unicaen.fr (V. Collot).

0968-0896/$ - see front matter © 2012 Elsevier Ltd. All rights reserved.
http://dx.doi.org/10.1016/j.bmc.2012.06.025

challenge for structure-based drug design. Nevertheless, several families of nNOS inhibitors have already been discovered. First, substrate analogues like L-arginine derivatives bearing a guanidine[2,4,21–23] or an amidine group,[2,4,24,25] sulphur analogues of L-citrulline[4,24] and isothioureas[4] have been synthesized, but despite the fact that some of these compounds appear as potent NOS inhibitors, none of them has showed a real selectivity towards nNOS. Then, heterocyclic inhibitors including imidazole[24] and indazole[26,27] derivatives have been developed revealing two corresponding lead compounds, the 1-((2-trifluoromethyl)phenyl)imidazole (TRIM)[4] and the 7-nitroindazole (7-NI).[4,10] Finally, Jaroch et al., Silverman et al. and Annedi et al. have recently respectively described in the literature some other promising new dihydroquinoleine[28], 2-aminopyridine[29] and indole[30,31] derivatives which appear as potent and above all for the last ones selective nNOS inhibitors.

In this context, considering the laboratory's know-how in indazole chemistry[32,33] and the interesting activity of 7-NI (IC_{50} = 0.71 μM)[26] which furthermore reveals a good in vivo selectivity towards nNOS, design, synthesis and pharmacological evaluation of new indazole libraries (Scheme 1) have been developed for a few years in our team in order to elucidate the structure–activity relationships of these compounds as nNOS inhibitors. Some results describing extensive pharmacomodulations realized on all positions of the indazole six-membered ring have already been published.[34–36] This large study has shown that many of 4- and 7-substituted derivatives appear as potent inhibitors in the opposite of 5- and 6-substituted ones. In this work, we have not only confirmed the interest of substitution in position 7 (7-NI, IC_{50} = 0.6 μM; 7-bromoindazole, IC_{50} = 14.3 μM), but also discovered a new family of potent nNOS inhibitors, the 4-substituted indazoles (4-nitroindazole (4-NI), IC_{50} = 3.1 μM; 4-bromoindazole, IC_{50} = 2.4 μM). In fact, these compounds had been until this time poorly investigated because of difficulties in chemical access.[36]

It is interesting to notice that all active 4- and 7-substituted similar compounds bear electron withdrawing groups and, above all, that these substituents can be considered as hydrogen bond acceptors. Thus, taking into account the analogous properties of these 4- and 7-nitro and haloindazoles, we report here a multidisciplinary study which aims to elucidate their binding mode in the nNOS active site. Firstly, nitrogenous fastening points on the indazole building block have been investigated referring to molecular modeling hypotheses and thanks to the in vitro biological evaluation of N_1- and N_2-methyl and ethyl-4-substituted indazoles on nNOS. Secondly, we attempted to confirm the importance of the substitution in position 4 or 7 by a hydrogen bond acceptor group thanks to the synthesis and the in vitro biological evaluation of a new analogous 4-substituted derivative, the 4-cyanoindazole.

2. Study of nitrogenous fastening points

2.1. Molecular modeling of 7-NI and 4-NI in the nNOS active site

Currently, several crystallographic data are available in the Protein Data Bank (PDB) presenting the NOSox co-crystallised with indazole derivatives.[37,38] All 3D structures show that these inhibitors don't directly bond as the substrate neither to the glutamic acid, nor to the heme iron of the active site. In the published 7-NI/iNOSox crystal structure as well as in the 7-NI/eNOSox one, two possible orientations of 7-NI were observed (Fig. 1).[38] In both cases, 7-NI stands parallel to the heme porphyrin ring with a π-stacking formation between them and the establishment of two hydrogen bonds. In the first majority orientation (named orientation A—Fig. 1), the nitro group of 7-NI interacts through a hydrogen bond with NH of Met 589 of the enzyme and the NH function in position 1 of the compound with carbonyl group of Trp 587. In the second orientation (named orientation B—Fig. 1), the nitro group interacts with NH of Gly 586 and the NH function in position 1 with carbonyl group of Trp 587.[40] However, a previously reported X-ray structure of 7-NI/nNOSox and 3-bromo-7-NI/NOSox complexes presented only the orientation A.[39] We have therefore based our modeling studies only on the orientation A.

The 7-NI/nNOS crystal model (orientation A) was energy minimized and this analysis showed that the binding energy of 7-NI with protein was about −28.8 kcal/mol. The energy minimization moved little the 7-NI towards Gly 586 ($RMSD_{heavy\ atoms}$ = 0.55 Å) and the enzyme backbone part interacting with 7-NI (from Phe 584 to Glu 590) changed only little ($RMSD_{heavy\ atoms}$ = 0.50 Å), principally a rearrangement in the hydrogen orientations was observed (Fig. 2). Moreover, the calculation of interaction energy with nNOS per 7-NI atom proved that crucial fastening points for recognition in the protein binding site were the oxygens of the nitro group (O_9 and O_{10}) and surprisingly the N_2 atom (Table 1). This is a contradictory result with respect to generally proposed 7-NI binding mode in NOS active site, in which the 7-NI is supposed to interact with the enzyme backbone through the oxygens of the nitro group, as we observed, but also through the NH function in position 1. Our study showed that the interaction energy of 7-NI H_1 atom with enzyme is near zero, contrary to the interaction energy of 7-NI N_2 atom which is one of the highest. Furthermore, the energy analysis on the 7-NI itself (from energy minimized complex) showed that the interaction exists between O_{10} and H_1 atoms. The calculated interaction energy between O_{10} and H_1 is about −21.12 kcal/mol and between O_{10} and N_1 about −17.06 kcal/mol. Then, a previous work on the X-ray structure of 7-NI itself published by our team revealed that the NH function of indazole was involved in an intramolecular hydrogen bond with one oxygen of the nitro group.[39] Thus, all these data showed that the NH function in position 1 of the indazole is involved in an intramolecular hydrogen bond with its nitro group also in the complex and it is therefore unlikely that this function be able to make at the same time another hydrogen bond with the protein backbone. Moreover, the visualization of minimized complex showed that N_2 of 7-NI was situated in the proximity of backbone Gly 586 NH group. The existence of a hydro-

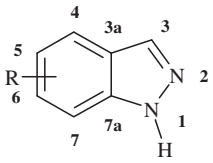

R = OMe, NO_2, F, Cl, Br, I...

Scheme 1. Pharmacomodulations recently described on the indazole six-membered ring.

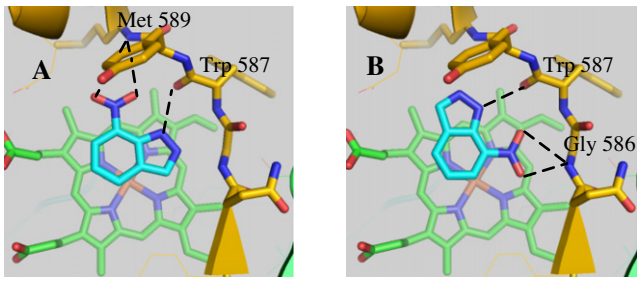

Figure 1. Structure of iNOSox co-crystallised with 7-NI with two different inhibitor orientations: orientation A in which the nitro group of 7-NI interacts with NH of Met 589 and orientation B in which it interacts with NH of Gly 586. Dashed lines indicate electrostatic interactions. This figure was made with PYMOL (DeLano Scientific, 2002, San Carlo, USA).

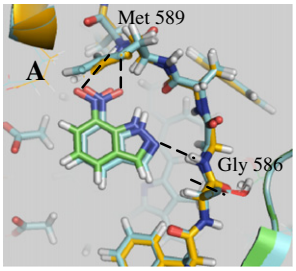

Figure 2. The superposition of 7-NI orientation A within the nNOS binding cavity before (7-NI in green and enzyme part in yellow) and after energy minimization (7-NI and enzyme part in cyan). Dashed lines indicate electrostatic interactions. This figure was made with PYMOL (DeLano Scientific, 2002, San Carlo, USA).

Table 1
Interaction energy between 7-NI, but also 4-NI and nNOS calculated per ligand atom. The strongest interactions (more negative values) are in bold

7-NI		4-NI	
Atom	Interaction energy (kcal/mol)	Atom	Interaction energy (kcal/mol)
C_{7a}	0.00	C_{3a}	0.00
N_1	2.32	C_3	1.16
H_1	0.19	H_3	1.64
N_2	**−17.74**	N_2	**−19.18**
C_3	0.91	N_1	3.80
H_3	1.95	H_1	5.04
C_{3a}	−1.05	C_{7a}	−3.51
C_4	−3.42	C_7	−3.27
H_4	2.84	H_7	3.14
C_5	−2.63	C_6	−2.40
H_5	1.91	H_6	1.56
C_6	−1.74	C_5	−1.59
H_6	−0.50	H_5	−0.84
C_7	0.44	C_4	0.50
N_8	12.93	N_8	13.91
O_9	**−9.04**	O_9	**−9.78**
O_{10}	**−13.13**	O_{10}	**−14.40**

gen bond of the N···NH type is possible and justifies the observed importance of the N_2 atom in the interaction with the protein (Fig. 2).

On the basis of these results, we propose that the 7-NI binding mode in nNOS active site is as follows: 7-NI interacts with the enzyme backbone through the oxygens of the nitro group and the N_2 atom.

Furthermore, the discovery of 4-NI efficiency as nNOS inhibitor strengthens this new suggested binding mode. Indeed, if the nitro group is conserved as a fixed fastening point, NH function in position 1 of 4-NI moves at the opposite side of the binding cavity without any contact with the protein backbone. Molecular docking studies were therefore carried out to position 4-NI in the heme binding cavity using Gold program.[40] The selected docking poses could be divided into two groups: one close to the orientation A of 7-NI and the second different to those observed for 7-NI (named orientation C—Figure 3).

Both complexes were submitted to energy minimization (Fig. 4). In the case of the 4-NI/nNOSox complex, the energy minimization turned slightly the 4-NI ($RMSD_{heavy\ atoms}$ = 0.55 Å) in the binding cavity for the solution A but changed globally the 4-NI orientation ($RMSD_{heavy\ atoms}$ = 2.47 Å) in the solution C. The changes in the interacting protein backbone concerned principally the hydrogen atoms for both solutions as in the case of the 7-NI/nNOSox complex ($RMSD_{heavy\ atoms}$ = 0.51 Å for solution A and $RMSD_{heavy\ atoms}$ = 0.41 Å for solution C). The comparison of the 4-NI/protein binding energy showed that it was the same level for orientations A (−25.2 kcal/mol) and C (−24.6 kcal/mol). However, the orientation C seems to be visually less likely since the nitro group doesn't interact with the protein and it was instable during the energy

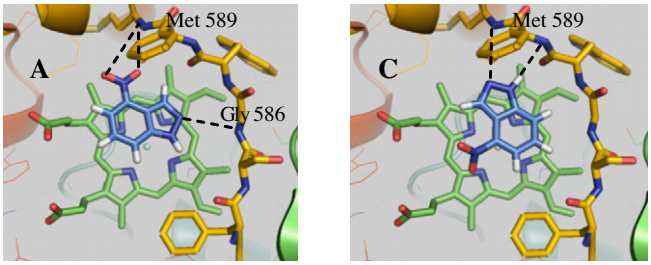

Figure 3. Two proposed orientations of 4-NI in the nNOS binding cavity from docking studies. Dashed lines indicate electrostatic interactions. This figure was made with PYMOL (DeLano Scientific, 2002, San Carlo, USA).

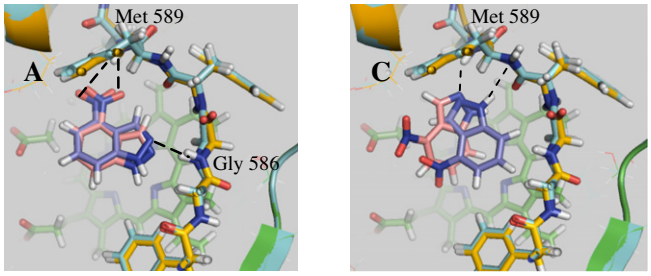

Figure 4. The superposition of 4-NI orientations A and C within the nNOS binding cavity before (4-NI in blue and enzyme part in yellow) and after energy minimization (4-NI in pink and enzyme part in cyan). This figure was made with PYMOL (DeLano Scientific, 2002, San Carlo, USA).

minimization ($RMSD_{heavy\ atoms}$ = 2.47 Å). After the energy minimization the 4-NI in solution C was deflected from coplanar orientation with respect to the heme and therefore the solution A was favoured (Fig. 4). Interestingly, the interaction energy analysis per 4-NI atom certified that 4-NI at orientation A reproduces the binding mode of 7-NI with three key interactions to the enzyme through the oxygen atoms of the nitro group as well as through the N_2 atom (Table 1). Then, looking at our modeling hypotheses, we observed that for orientation A there is a possibility to put a larger substituent, like a methyl group, on the N_1 atom, but in the orientation C this substitution is not conceivable. Furthermore, for orientation A N_2-substituted derivatives should appear as less potent nNOS inhibitors losing a possibility of hydrogen bond. Thus, for a better understanding of 4-substituted indazole binding in the nNOS active site and to confirm the new modeling hypotheses, synthesis and in vitro pharmacological evaluation of 1- and 2-alkyl 4-substituted indazole derivatives have been developed.

2.2. Synthesis and in vitro biological evaluation of N_1- and N_2-methyl and ethyl-4-substituted indazoles 3–6

In this context, we directly managed to prepare, thanks to the indazole-ring prototropic tautomery, 1- and 2-methyl-4-nitroindazoles **3a–b**, but also 1- and 2-methyl-4-bromoindazoles **5a–b** nearly in a ratio of two thirds to one third starting respectively from 4-nitro and 4-bromoindazoles **1** and **2a** in the presence of iodomethane and potassium carbonate in acetone reflux[41] (Scheme 2, Table 2). Similarly, 1- and 2-ethyl-4-nitroindazoles **4a–b** and 1- and 2-ethyl-4-bromoindazoles **6a–b** have been synthesized in good yields replacing iodomethane by iodoethane (Scheme 2, Table 2). We can notice that Cheung et al. reported in 2003 a regioselective methylation of indazole derivatives in position 2 using trimethyloxonium tetrafluoroborate as alkyling agent.[42] However, we chose to use a more classic method to obtain, after a simple separation by chromatography, the both expected 1- and 2-substituted compounds. Moreover, each of these products

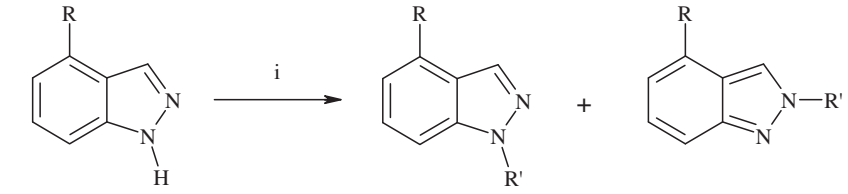

R = NO_2 (**1**) or Br (**2a**) R' = CH_3 or C_2H_5

3-6

Scheme 2. Reagents and conditions: (i) CH_3I or C_2H_5I (1.2–1.8 equiv), K_2CO_3 (3 equiv), acetone, reflux, 3–8 h, 35–69%.

Table 2
N_1 and N_2-alkylation of 4-nitro and 4-bromoindazoles

R	R′		Total yield (%)	Ratio (%)
4-NO_2	N_1-CH_3	**3a**	60	59
	N_2-CH_3	**3b**		41
	N_1-C_2H_5	**4a**	57	65
	N_2-C_2H_5	**4b**		35
4-Br	N_1-CH_3	**5a**	69	68
	N_2-CH_3	**5b**		32
	N_1-C_2H_5	**6a**	35	57
	N_2-C_2H_5	**6b**		43

has been identified thanks to X-ray crystallography studies realized in our laboratory (Fig. 5).

Effects of these different indazole derivatives on nNOS activity were evaluated in vitro according to a procedure described in the experimental section. N_1-alkyl-4-substituted indazoles **3a**, **4a**, **5a** and **6a** appeared as less potent nNOS inhibitors than 4-nitro and 4-bromoindazoles, but remained active in contrast to N_2-alkyl-4-substituted indazoles **3b**, **4b**, **5b** and **6b** (Table 3). Thus, the NH function at position 1 doesn't seem to be essential for 4-substituted indazole binding with the enzyme, but the substitution at this point isn't always very well-tolerated considering the nNOS activity especially with bulky groups. Indeed, N_1-ethyl-4-substituted indazoles **4a** and **6a** are less efficient nNOS inhibitors than N_1-methyl-4-substituted indazoles **3a** and **5a** (Table 3). Therefore, these results allow us to reject the orientation C proposed by docking (Fig. 3). Moreover, N_2 indisponibility for binding due to its obstruction by alkyl group leads on the contrary to the complete loss of inhibitory activity which makes of this nitrogen a crucial fastening point. In fact, the similar potency of 7-NI and 4-NI as nNOS inhibitors only seems to be conceivable thanks to this common fastening point which allows the rotation of the nitro group for both compounds to the correct position. We have also discovered in the litterature[26,27] that N_1- and N_2-methyl-7-nitroindazoles are poor nNOS inhibitors what proves another time the importance of the nitrogen in position 2 in the binding. The N_1-methyl derivative would just be here too much clustered to have a good affinity

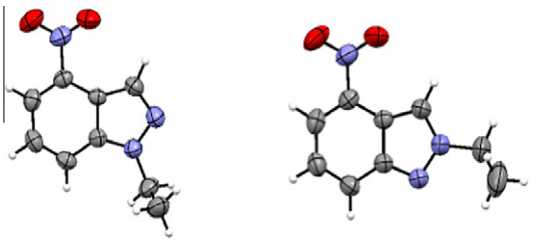

Figure 5. ORTEP diagram of the X-ray structure of 1- and 2-ethyl-4-nitroindazoles (**4a**–**b**) with the thermal ellipsoid at 50% probability.

Table 3
IC_{50} values of N_1- and N_2-alkyl-4-substituted indazoles and 4-cyanoindazole against rat cerebellar nNOS

Indazole derivative	IC_{50} (μM) mean ± sem	Inhibition at 100 μM (%)	Vehicle	Number of experiments
3a	10.6 ± 4.2	86	DMSO 0.4%	7
3b	>100	34	DMSO 0.4%	6
4a	51.7 ± 22.3	67	DMSO 0.4%	4
4b	>100	34	DMSO 0.4%	3
5a	28.2 ± 7.1	75	DMSO 0.4%	3
5b	>100	19	DMSO 0.4%	3
6a	72.5 ± 27.5	61	DMSO 0.4%	3
6b	>100	0	DMSO 0.4%	3
9a	42.5 ± 2.5	63	DMSO 0.4%	3

(Fig. 2). On the contrary, the methyl group in position 1 of the 4-NI corresponding compound seems to have enough place to be accepted (Fig. 3). Finally, all these biological data confirm the new modeling hypotheses and demonstrate that 4-substituted indazoles as well as 7-NI bind to the nNOS active site through the orientation A (Figs. 2 and 3): crucial role in their binding is played by the N_2 atom and not by the NH function at position 1 as it was previously proposed.[26,27,35]

3. Introduction of a new hydrogen bond acceptor group in position 4

3.1. Synthesis and in vitro biological evaluation of 4-cyanoindazole 9a

All the already described potent nNOS inhibitor indazole derivatives bear a hydrogen bond acceptor substituent in position 4 or 7. As we have previously demonstrated thanks to the molecular modeling studies, this substituent appears essential for their binding. For the halogen derivatives, it was recently observed that halogens are able to establish two kinds of contacts in biomolecular systems: C-X···O and C–X···H.[43,44] Therefore, we can assume that halogens play a role of hydrogen bond acceptors, like the nitro group, in our system.

To develop the 4-substituted indazole new nNOS inhibitor family and to replace the methemoglobinisant and carcinogenic nitro group of 4-NI, we aimed to synthesize the 4-cyanoindazole also bearing a hydrogen bond acceptor substituent. Indeed, Cottyn et al. have already proved the interest of 7-cyanoindazole as nNOS

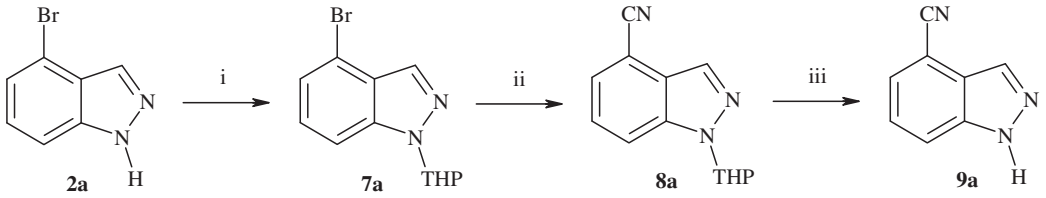

Scheme 3. Reagents and conditions: (i) DHP (2.5 equiv), TFA (cat.), EtOAc, reflux, 6 h, 82%; (ii) $Zn(CN)_2$ (1.13 equiv), $Pd_2(dba)_3$ (0.04 equiv), *S*-Phos (0.1 equiv), DMF/water 99:1, microwave heating at 150 °C, 40 min, 79%; (iii) EtOH–HCl, rt, 3 h, 76%.

inhibitor (IC_{50} = 25 μM).[27] However, this compound didn't appear as potent as 7-NI that's why we tried to use the analogy between 4- and 7-substituted indazoles to design a more efficient derivative. Taking into account the laboratory's know-how in metal-catalysed cross coupling reactions,[32,33] a new palladium-catalysed cyanation procedure has been carried out from haloindazoles and using microwave heating to reduce reaction time comparing to the described synthesis of 7-cyanoindazole. In fact, we first adapted the isoquinoleine cyanation method reported by Chobanian et al. in 2006[45] to 5-bromoindazole **2b** because of the usually better reactivity of position 5. Unfortunately, by reacting with zinc cyanide, $Pd_2(dba)_3$ as the catalyst and S-Phos as the ligand in DMF-water 99:1 at 150 °C in a microwave reactor for 40 min, we only obtained 5-cyanoindazole with a 22% yield. However, we suggested that the unprotected NH group could poison the catalyst by complexation with the palladium. Thus, thanks to a previously described work about indazole protection by a tetrahydropyran-2-yl (THP) group[32,33] a new assay starting from 1-THP-5-bromoindazole **7b** could be realized and offered the corresponding cyano derivative **8b** with an excellent yield of 79%. Then, the same reaction conditions were applied to 1-THP-4-bromoindazole **7a** also with a very good yield of 79%. Finally, we obtained the expected unprotected 4- and 5-cyanoindazoles **9a–b** with a respective yield of 76% and 79% using a treatment with ethanolic HCl at room temperature already reported by our team for similar deprotections of other indazole derivatives (Scheme 3).[33]

As shown in Table 3, 4-cyanoindazoles (**9a**) displayed a modest inhibitory effect against NOS activity. However, this data confirmed at least the already suggested importance of indazole nucleus substitution by hydrogen bond acceptor groups at position 4. With this in mind, molecular modeling studies were finally carried out considering this new indazole derivative to analyze the potential similarities with other 4-substituted indazole binding mode.

Table 4
Interaction energy between 4-cyanoindazole **9a** and nNOS calculated per ligand atom. The strongest interactions (more negative values) are in bold.

4-Cyanoindazole	
Atom	Interaction energy (kcal/mol)
C_{7a}	0.00
N_1	1.10
H_1	1.50
N_2	**−18.24**
C_3	3.48
H_3	4.66
C_{3a}	−3.84
C_4	−3.65
H_4	3.04
C_5	−3.12
H_5	2.53
C_6	−2.19
H_6	0.11
C_7	0.05
C_8	6.20
N_9	**−17.50**

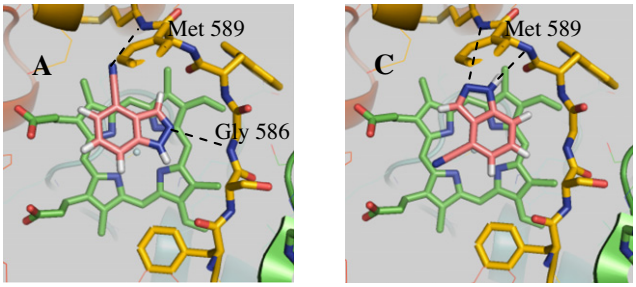

Figure 6. Two proposed orientations of 4-cyanoindazole in the nNOS binding cavity from docking studies. Dashed lines indicate electrostatic interactions. This figure was made with PYMOL (DeLano Scientific, 2002, San Carlo, USA).

3.2. Molecular modeling of 4-cyanoindazole in the nNOS active site

As in the case of 4-NI, docking studies of 4-cyanoindazole in the nNOS active site proposed two orientations: one analogous to the orientation A of 7-NI and the second close to the orientation C already observed with 4-NI (Fig. 6). The 4-cyanoindazole/nNOSox interaction energy is approximately the same level for both orientations with about a difference of 5 kcal/mol in benefit of the orientation C. However, in the orientation C the cyano group doesn't participate in the interaction with the protein. Therefore, by analogy with 4-NI binding mode we can assume that the orientation C be again excluded. The energy minimization turned slightly the 4-cyanoindazole in a similar way to orientation A of 4-NI/nNOSox complex. The interaction energy with protein calculated per 4-cyanoindazole atom for the orientation A showed that the N_2 atom and the nitrogen of cyano group (N_9) participated strongly in the fixation (Table 4). Indeed, hydrogen bond type interactions were observed between N_2 and NH of Met 589 (d_{N-N} ≈2.99 Å) and the nitrogen of cyano group and NH of Gly 586 (d_{N-N} ≈3.21 Å). Finally, in the orientation A, the 4-cyanoindazole is able to reproduce the two attachment points observed with 7-NI and 4-NI. These last results confirm the new molecular modeling hypotheses for the binding of 4 and 7-substituted indazoles: the N_2 atom and the substitution in position 4 or 7 by a hydrogen bond acceptor group play a crucial role for their interaction with nNOS.

4. Conclusion

To conclude, several advances have been made in the study of 4-substituted indazoles as potent neuronal nitric oxide synthase inhibitors. Firstly, this multidisciplinary work allowed us to elucidate the binding mode of these indazole derivatives as well as of 7-NI in the nNOS active site. Indeed, by opposition to previous hypotheses[26,27,35,37,38] describing the NH function in position 1 of the indazole as a key fastening point, the present study speaks in favour of a crucial role of the nitrogen in position 2. Secondly, the interest of substitution at position 4 by a hydrogen bond acceptor has been confirmed thanks not only to the synthesis and the

in vitro biological evaluation of a new compound in this series, the 4-cyanoindazole, but also by molecular modeling studies. Taking into account these new data, advanced structure-activity relationship studies could be performed in the future to explore notably the substitution in position 1 of 4-substituted indazoles since 3-bromo-7-NI appears in the litterature, by analogy, as a potent nNOS inhibitor (IC_{50} = 0.17 μM).[26]

5. Experimental section

5.1. Chemistry

All commercial reagents were used as received without further purification. Reaction mixtures were stirred magnetically and monitored by TLC using 0.2 mm *Macherey-Nagel Polygram SIL G/UV$_{254}$* precoated plates. Column chromatography was performed using *CarloErba-SDS 60A 70–200 μm* silica gel. Melting points were determinated on a Köfler melting point apparatus. IR spectra were taken with a *Perkin-Elmer spectrum X FT-IR* spectrometer. ^{1}H NMR (400 MHz) and ^{13}C NMR (100 MHz) spectra were recorded on a *JEOL Lambda 400* spectrometer. Chemical shifts (δ) are expressed in parts per million downfield from tetramethylsilane as an internal standard and the coupling constants are in Hertz. High and low resolution electron impact (EI) mass spectra were recorded on a *JEOL JMS GCMate* spectrometer with ionising potential of 70 eV and with pfk as internal standard. Low resolution electrospray (ESI) mass spectra were obtained on a LC/MS *Waters alliance 2695* with a *Xterra MSC 118/2,1 × 50 mm* column coupled with a *Micromass ZMD 2000* spectrometer. Elemental analyses were performed at the 'Institut de Recherche en Chimie Organique Fine' (Rouen, France).

Single crystals of compounds **4a–b** suitable for X-ray crystallographic analysis were obtained by slow evaporation from cyclohexane. Data for crystal structure analysis were collected at 296 K with a Bruker-Nonius Kappa CCD area detector diffractometer with graphite-monochromatized Mo K_λ radiation (λ = 0.71073 Å). The structure was solved using direct methods and refined by full-matrix least-squares analysis on F^2. Program used to solve and refine structure: SHELXS-97. Software used to prepare material for publication: SHELXL-97.[46]

5.1.1. General procedure for the synthesis of 4-nitro and 4-bromo-1*H*-indazoles (1 and 2a)[36]

To a cooled solution of the chosen 2-methylaniline dissolved in HBF_4 (50% solution in water; 15–30 mL) was added at 0 °C dropwise a cooled aqueous solution of $NaNO_2$ (1 equiv in the minimum of water). After the end of the addition, the mixture was stirred 1 h at 0 °C and 2 h at room temperature. Then, the resulting precipitate was filtered, washed with Et_2O (3 × 100 mL) and dried to obtain the corresponding 2-methylphenyldiazonium tetrafluoroborate salts which were directly added in one portion under nitrogen to a stirred mixture of KOAc (2 equiv) and 18-crown-6 (0.05 equiv) in dry $CHCl_3$ (350–700 mL). After 2 h at room temperature, the mixture was filtered, washed with $CHCl_3$ (3 × 100 mL) and the organic filtrate was finally concentrated in vacuo. The residual gum was purified by column chromatography on silica gel (EtOAc/cyclohexane 1:3) to give the desired indazoles **1** and **2a**.

5.1.1.1. 4-Nitro-1*H*-indazole (1). Starting from the 3-nitro-2-methylaniline (10 g, 65.7 mmol) and respecting the general procedure the 3-Nitro-2-methylphenyldiazonium tetrafluoroborate salt (11.7 g, 46.6 mmol) was first obtained, followed by the expected product **1** as a brown solid (6.8 g, 63% for two steps). Mp 207 °C. TLC R_f = 0.09 (Silica gel; EtOAc/cyclohexane 2:3). IR (KBr): 3311, 1518, 1337, 1239, 942, 738 cm^{-1}. ^{1}H NMR (DMSO-d_6) δ: 7.62 (t, *J* = 7.9 Hz, 1H), 8.10 (d, *J* = 8.3 Hz, 1H), 8.17 (d, *J* = 7.6 Hz, 1H), 8.54 (s, 1H), 13.92 (s, 1H). ^{13}C NMR (DMSO-d_6) δ: 115.3, 118.3, 118.5, 125.7, 132.5, 139.7, 141.6. HRMS/EI *m/z* calcd for $C_7H_5N_3O_2$ [M]$^+$: 163.0382; found: 163.0386.

5.1.1.2. 4-Bromo-1*H*-indazole (2a). Starting from the 3-bromo-2-methylaniline (5.9 g, 31.7 mmol) and respecting the general procedure, the 3-bromo-2-methylphenyldiazonium tetrafluoroborate salt (9.1 g, 31.4 mmol) was first obtained, followed by the expected product **2a** as a brown solid (3.6 g, 57% for two steps). Mp 170 °C. TLC R_f = 0.24 (Silica gel; EtOAc/cyclohexane 1:3). IR (KBr): 3438, 3142, 3048, 2857, 1621, 1354, 1183, 965, 916, 769 cm^{-1}. ^{1}H NMR ($CDCl_3$) δ: 7.23 (t, *J* = 10.7 Hz, 1H), 7.33 (d, *J* = 7.8 Hz, 1H), 7.46 (d, *J* = 7.8 Hz, 1H), 8.12 (s, 1H), 10.75 (s, 1H). ^{13}C NMR ($CDCl_3$) δ: 108.8, 114.6, 124.0, 124.5, 127.6, 135.1, 140.6. LRMS/EI *m/z (%)*: 199 (2.8), 198 (M$^+$, 1.97), 197 (9), 196 (M$^+$, 100), 117 (23). Anal. calcd for $C_7H_5BrN_2$ (%): C, 42.67; H, 2.56; N, 14.22; found: C, 42.76; H, 2.34; N, 13.82.

5.1.2. General procedure for the synthesis of 1- and 2-methyl-4-nitro and 4-bromo-1*H*-indazoles (3a–b and 5a–b)

To a solution of potassium carbonate (3 equiv) in acetone (15-30 mL) was added the chosen 4-substituted indazole **1** or **2a** and the mixture was stirred for 30 min at room temperature. Then, methyl iodide (1.2–1.8 equiv) was finally introduced in the reaction mixture which was heated under reflux conditions for 3–8 h. After evaporating acetone, the residue was dissolved in EtOAc (30 mL) and the organic layer was washed with brine (3 × 15 mL), dried over $MgSO_4$, filtered and evaporated in vacuo. The crude material was purified by flash column chromatography on silica gel (EtOAc/cyclohexane, 1:2 or CH_2Cl_2) to give the expected 1- and 2-methyl-4-substituted-indazoles **3a**–**b** and **5a–b**.

5.1.2.1. 1-Methyl-4-nitro-1*H*-indazole (3a). Starting from the 4-nitro-1*H*-indazole **1** (0.5 g, 3.1 mmol) and following the general procedure with a purification by flash column chromatography on silica gel thanks to CH_2Cl_2, the product **3a** was obtained as a yellow solid (0.2 g, 35%). Mp 145 °C. TLC R_f = 0.28 (Silica gel; CH_2Cl_2). IR (KBr): 1513, 1341, 1324, 1267, 999, 963, 808, 738, 729 cm^{-1}. ^{1}H NMR ($CDCl_3$) δ: 4.18 (s, 3H), 7.52 (t, *J* = 7.8 Hz, 1H), 7.77 (d, *J* = 7.8 Hz, 1H), 8.16 (d, *J* = 7.8 Hz, 1H), 8.61 (s, 1H). ^{13}C NMR ($CDCl_3$) δ: 35.0, 114.9, 115.9, 117.0, 124.2, 131.5, 139.6, 140.4. LRMS/ESI: [M+H]$^+$ 178. HRMS/EI *m/z* calcd for $C_8H_7N_3O_2$ [M]$^+$: 177.0538; found: 177.0537.

5.1.2.2. 2-Methyl-4-nitro-1*H*-indazole (3b). Starting from the 4-nitro-1*H*-indazole **1** (0.5 g, 3.1 mmol) and following the general procedure with a purification by flash column chromatography on silica gel thanks to CH_2Cl_2, the product **3b** was obtained as a yellow solid (0.1 g, 25%). Mp 110 °C. TLC R_f = 0.31 (Silica gel; CH_2Cl_2). IR (KBr): 2927, 1522, 1338, 1280, 1153, 783 cm^{-1}. ^{1}H NMR ($CDCl_3$) δ: 4.32 (s, 3H), 7.41 (t, *J* = 7.8 Hz, 1H), 8.08 (d, *J* = 8.8 Hz, 1H), 8.19 (d, *J* = 7.8 Hz, 1H), 8.56 (s, 1H). ^{13}C NMR ($CDCl_3$) δ: 40.9, 115.1, 120.6, 124.3, 125.2, 125.8, 140.6, 150.0. LRMS/ESI: [M+H]$^+$ 178. LRMS/EI *m/z* (%): 178 (13), 177 (M$^+$, 100), 131 (40), 116 (5). HRMS/EI *m/z* calcd for $C_8H_7N_3O_2$ [M]$^+$: 177.0538; found: 177.0530.

5.1.2.3. 1-Methyl-4-bromo-1*H*-indazole (5a). Starting from the 4-bromo-1*H*-indazole **2a** (0.5 g, 2.5 mmol) and following the general procedure with a purification by flash column chromatography on silica gel thanks to EtOAc/cyclohexane, 1:2, the product **5a** was obtained as an orange oil (0.2 g, 47%). TLC R_f = 0.54 (Silica gel; EtOAc/cyclohexane, 1:2). IR (KBr): 1615, 1561, 1494, 1432, 1262, 1187, 1114, 989, 915; 830, 770, 730, 627 cm^{-1}. ^{1}H NMR ($CDCl_3$) δ: 4.08 (s, 3H), 7.24 (t, *J* = 6.8 Hz, 1H), 7.30 (d, *J* = 6.8 Hz,

1H), 7.35 (d, J = 7.8 Hz, 1H), 8.00 (s, 1H).^{13}C NMR ($CDCl_3$) δ: 34.9, 107.0, 113.6, 122.3, 124.0, 126.0, 131.8, 139.4. LRMS/ESI: $[M+H]^+$ 211 and 213. HRMS/EI m/z calcd for $C_8H_7BrN_2$ $[M]^+$: 209.9793; found: 209.9790.

5.1.2.4. 2-Methyl-4-bromo-1*H*-indazole (5b). Starting from the 4-bromo-1*H*-indazole **2a** (0.5 g, 2.5 mmol) and following the general procedure with a purification by flash column chromatography on silica gel thanks to EtOAc/cyclohexane, 1:2, the product **5b** was obtained as a brown oil (0.1 g, 22%). TLC R_f = 0.25 (Silica gel; EtOAc/cyclohexane, 1:2). IR (KBr): 2944, 1625, 1534, 1400, 1369, 1283, 1190, 1157, 936, 770 cm^{-1}. ^{1}H NMR ($CDCl_3$) δ: 4.24 (s, 3H), 7.14 (t, J = 6.8 Hz, 1H), 7.24 (d, J = 6.8 Hz, 1H), 7.63 (d, J = 8.8 Hz, 1H), 7.93 (s, 1H). ^{13}C NMR ($CDCl_3$) δ: 40.5, 112.7, 116.5, 124.1, 124.2, 124.6, 126.6, 148.9. LRMS/ESI: $[M+H]^+$ 211 and 213. HRMS/EI m/z calcd for $C_8H_7BrN_2$ $[M]^+$: 209.9793; found: 209.9783.

5.1.3. General procedure for the synthesis of 1- and 2-ethyl-4-bromo and 4-nitro-1*H*-indazoles (4a–b and 6a–b)

To a solution of potassium carbonate (3 equiv) in acetone (15–30 mL) was added the chosen 4-substituted indazole **1** or **2a** and the mixture was stirred for 30 min at room temperature. Then, ethyl iodide (1.2–1.8 equiv) was finally introduced in the reaction mixture which was heated under reflux conditions for 3–8 h. After evaporating acetone, the residue was dissolved in EtOAc (30 mL) and the organic layer was washed with brine (3 × 15 mL), dried over $MgSO_4$, filtered and evaporated in vacuo. The crude material was purified by flash column chromatography on silica gel (EtOAc/cyclohexane, 1:2 or CH_2Cl_2) to give the expected 1- and 2-ethyl-4-substituted-indazoles **4a**–**b** and **6a–b**.

5.1.3.1. 1-Ethyl-4-nitro-1*H*-indazole (4a). Starting from the 4-nitro-1*H*-indazole **1** (0.5 g, 3.1 mmol) and following the general procedure with a purification by flash column chromatography on silica gel thanks to CH_2Cl_2, the product **4a** was obtained as a yellow solid (0.2 g, 37%). Mp 119 °C. TLC R_f = 0.35 (Silica gel; CH_2Cl_2). IR (KBr): 2978, 1522, 1336, 1289, 1197, 1027, 951, 804, 788, 738 cm^{-1}. ^{1}H NMR ($CDCl_3$) δ: 1.57 (t, J = 7.0 Hz, 3H, CH_3), 4.48 (q, J = 7.8 Hz, 2H), 7.50 (t, J = 8.8 Hz, 1H), 7.79 (d, J = 7.8 Hz, 1H), 8.14 (d, J = 6.8 Hz, 1H), 8.61 (s, 1H). ^{13}C NMR ($CDCl_3$) δ: 15.0, 44.4, 116.0, 117.1, 118.1, 125.2, 132.6, 140.6, 140.8. LRMS/ESI: $[M+H]^+$ 192. LRMS/EI m/z (%): 192 (23), 191 (M^+, 100), 190 (4), 177 (17), 176 (100), 163 (24), 146 (5), 145 (36), 144 (6), 133 (15), 131 (6), 130 (53), 129 (8), 119 (25), 118 (27), 117 (20), 116 (9), 105 (15), 103 (16), 102 (11). HRMS/EI m/z calcd for $C_9H_9N_3O_2$ $[M+H]^+$: 192,0773; found: 192,0776.

5.1.3.2. 2-Ethyl-4-nitro-1*H*-indazole (4b). Starting from the 4-nitro-1*H*-indazole **1** (0.5 g, 3.1 mmol) and following the general procedure with a purification by flash column chromatography on silica gel thanks to CH_2Cl_2, the product **4b** was obtained as a yellow solid (0.1 g, 20%). Mp 84 °C. TLC R_f = 0.28 (Silica gel; CH_2Cl_2). IR (KBr): 1521, 1499, 1429, 1340, 1295, 1235, 1149, 797, 737 cm^{-1}. ^{1}H NMR ($CDCl_3$) δ: 1.70 (t, J = 6.8 Hz, 3H), 4.57 (q, J = 6.8 Hz, 2H), 7.40 (t, J = 7.8 Hz, 1H), 8.09 (d, J = 8.8 Hz, 1H), 8.18 (d, J = 7.8 Hz, 1H), 8.58 (s, 1H). ^{13}C NMR ($CDCl_3$) δ: 15.7, 49.2, 114.9, 120.5, 123.6, 124.2, 125.9, 140.6, 149.8. LRMS/ESI: $[M+H]^+$ 192. LRMS/EI m/z (%): 192 (11), 191 (M^+, 100), 176 (18), 163 (39), 145 (12), 133 (14), 105 (10). HRMS/EI m/z calcd for $C_9H_9N_3O_2$ $[M]^+$: 191.0695; found: 191.0693.

5.1.3.3. 1-Ethyl-4-bromo-1*H*-indazole (6a). Starting from the 4-bromo-1*H*-indazole **2a** (1 g, 5.1 mmol) and following the general procedure with a purification by flash column chromatography on silica gel thanks to EtOAc/cyclohexane, 1:2, the product **6a** was obtained as an orange oil (0.2 g, 20%). TLC R_f = 0.42 (Silica gel; EtOAc/cyclohexane, 1:3). IR (KBr): 2980, 1612, 1560, 1492, 1447, 1363, 1292, 1177, 1122, 915, 828, 770, 731 cm^{-1}. ^{1}H NMR ($CDCl_3$) δ: 1.50 (t, J = 6.8 Hz, 3H), 4.41 (q, J = 6.8 Hz, 2H), 7.20 (t, J = 7.8 Hz, 1H), 7.27 (d, J = 6.8 Hz, 1H), 7.33 (d, J = 7.8 Hz, 1H), 8.00 (s, 1H).^{13}C NMR ($CDCl_3$) δ: 14.8, 44.1, 108.0, 114.7, 123.2, 125.1, 126.8, 132.8, 139.5. LRMS/ESI: $[M+H]^+$ 225 and 227. LRMS/EI m/z (%): 226 (M^+, 73), 224 (M^+, 75), 213 (100), 212 (94), 205 (42), 161 (73), 146 (29). HRMS/EI m/z calcd for $C_9H_9BrN_2$ $[M]^+$: 225,0027; found: 225,0023.

5.1.3.4. 2-Ethyl-4-bromo-1*H*-indazole (6b). Starting from the 4-bromo-1*H*-indazole **2a** (1 g, 5.1 mmol) and following the general procedure with a purification by flash column chromatography on silica gel thanks to EtOAc/cyclohexane, 1:2, the product **6b** was obtained as an orange oil (0.2 g, 15%). TLC R_f = 0.35 (Silica gel; EtOAc/cyclohexane, 1:3). IR (KBr): 2982, 1625, 1533, 1444, 1413, 1371, 1294, 1188, 1153, 932, 769 cm^{-1}. ^{1}H NMR ($CDCl_3$) δ: 1.62 (t, J = 6.8 Hz, 3H), 4.44 (q, J = 6.8 Hz, 2H), 7.12 (t, J = 6.8 Hz, 1H), 7.22 (d, J = 6.8 Hz, 1H), 7.64 (d, J = 8.8 Hz, 1H), 7.92 (s, 1H). ^{13}C NMR ($CDCl_3$) δ: 15.6, 48.6, 112.7, 116.5, 122.8, 123.7, 124.0, 126.4, 148.6. LRMS/ESI: $[M+H]^+$ 225 and 227. LRMS/EI m/z (%): 226 (M^+, 93), 224 (M^+, 100), 198 (52), 196 (55). Anal. calcd for $C_9H_9BrN_2$ (%): C, 48.03; H, 4.03; Br, 35.50; N, 12.45; found: C, 48.26; H, 4.15; Br, 35.83; N, 12.40.

5.1.4. General procedure for the synthesis of 4 and 5-bromo-1-(tetrahydro-2*H*-pyran-2-yl)-1*H*-indazoles (7a–b) [32]

The chosen bromoindazole **2a–b** dissolved in ethyl acetate or chloroform (20 mL), a catalytic amount of TFA and 3,4-dihydro-2*H*-pyrane (2.5 equiv) were heated under reflux conditions for 6 h. Then, the solution was concentrated in vacuo and EtOAc (40 mL) was added to the residue. The organic layer was successively washed with a satured potassium carbonate solution (3 × 20 mL) and brine (3 × 20 mL), dried over $MgSO_4$, filtered and evaporated in vacuo. The crude material was purified by flash column chromatography on silica gel (EtOAc/cyclohexane, 1:4) to give the expected 1-THP-bromoindazoles **7a–b**.

5.1.4.1. 4-Bromo-1-(tetrahydro-2*H*-pyran-2-yl)-1*H*-indazole (7a). Starting from the 4-bromo-1*H*-indazole **2a** (2 g, 10.1 mmol) and following the general procedure in ethyl acetate, the product **7a** was obtained as a brown solid (2.3 g, 82%). Mp 72 °C. TLC R_f = 0.50 (Silica gel; EtOAc/cyclohexane 1:3). IR (KBr): 3435, 2963, 2944, 2850, 2866, 1611, 1567, 1493, 1446, 1418, 1249, 1170, 1079, 1059, 1040, 914, 772 cm^{-1}. ^{1}H NMR ($CDCl_3$) δ: 2.18-2.22 (m, 5H), 2.50-2.56 (m, 1H), 3.71-3.77 (m, 1H), 4.00-4.07 (m, 1H), 5.72 (dd, J = 6.6 Hz and J' = 2.7 Hz, 1H), 7.24 (t, J = 8.1 Hz, 1H), 7.32 (d, J = 7.3 Hz, 1H), 7.55 (d, J = 8.3 Hz, 1H), 8.04 (s, 1H). ^{13}C NMR ($CDCl_3$) δ: 22.4, 25.1, 29.4, 67.4, 85.7, 109.4, 114.5, 124.1, 125.5, 127.4, 133.9, 141.1. LRMS/EI m/z (%): 283 (38), 281 (M^+, 38), 240 (98), 238 (100), 196 (21), 117 (21). HRMS/EI m/z calcd for $C_{12}H_{13}BrN_2O$ $[M]^+$: 280.0211; found: 280.022.

5.1.4.2. 5-Bromo-1-(tetrahydro-2*H*-pyran-2-yl)-1*H*-indazole (7b). Starting from the 5-bromo-1*H*-indazole **2b** (0.7 g, 3.7 mmol) and following the general procedure in chloroform, the product **7b** was obtained as an orange oil (0.7 g, 70%). TLC R_f = 0.35 (Silica gel; EtOAc/cyclohexane 1:8). IR (KBr): 3429, 3100, 2942, 2859, 1733, 1611, 1486, 1441, 1418, 1275, 1210, 1179, 1116, 1082, 1043, 994, 910, 801, 783 cm^{-1}. ^{1}H NMR ($CDCl_3$) δ: 1.75-1.77 (m, 3H), 2.07-2.09 (m, 2H), 2.50-2.52 (m, 1H), 3.72-3.77 (m, 1H), 4.00-4.03 (m, 1H), 5.69 (dd, J = 6.6 Hz and J' = 2.7 Hz, 1H), 7.46 (dd, J = 8.1 Hz and J' = 1.7 Hz, 1H), 7.50 (d, J = 8.8 Hz, 1H), 7.87 (d, J = 1.7 Hz, 1H), 7.96 (s, 1H). ^{13}C NMR ($CDCl_3$)

δ: 22.4, 25.1, 29.3, 67.4, 85.5, 111.7, 114.3, 123.4, 126.2, 129.6, 133.0, 138.2. LRMS/EI *m/z (%)*: 282 (M^+, 9), 280 (M^+, 9), 198 (73), 196 (77), 117 (24), 90 (26), 85 (100), 84 (85), 76 (13). HRMS/EI *m/z* calcd for $C_{12}H_{13}BrN_2O$ $[M]^+$: 280.0211; found: 280.0198.

5.1.5. General procedure for the synthesis of 1-(tetrahydro-2*H*-pyran-2-yl)-1*H*-indazole-4 and 5-carbonitriles (8a–b)

The chosen 1-THP-bromoindazole **7a–b** dissolved in DMF/water 99:1 (5 mL), SPhos (0.1 equiv), $Pd_2(dba)_3$ (0.04 equiv) and zinc cyanide (1.13 equiv) were combined in a microwave tube fitted with a crimped septum cap. The tube was evacuated and then filled with argon and stirred at room temperature for 15 min. The reaction mixture was heated in a microwave at 150 °C for 40 min. After evaporating DMF in vacuo, EtOAc (30 mL) was added to the residue and the organic layer was successively washed with a 1 N sodium hydroxide solution (3 × 15 mL) and brine (3 × 15 mL), dried over $MgSO_4$, filtered and concentrated in vacuo. The crude material was purified by flash column chromatography on silica gel (EtOAc/cyclohexane, 1:4 to 1:3) to give the attempted 1-THP-indazole-carbonitriles **8a-b**.

5.1.5.1. 1-(Tetrahydro-2*H*-pyran-2-yl)-1*H*-indazole-4-carbonitrile (8a). Starting from the 4-bromo-1-(tetrahydro-2*H*-pyran-2-yl)-1*H*-indazole **7a** (0.3 g, 1 mmol) and following the general procedure, the product **8a** was obtained as a yellow solid (0.2 g, 79%). Mp 88 °C. TLC R_f = 0.28 (Silica gel; EtOAc/cyclohexane 1:4). IR (KBr): 2913, 2855, 2226, 1604, 1449, 1374, 1225, 1080, 1037, 967, 916, 787 cm^{-1}. ^1H NMR ($CDCl_3$) δ: 1.69–1.81 (m, 3H), 2.04–2.14 (m, 2H), 2.49–2.55 (m, 1H), 3.76 (t, J = 7.8 Hz, 1H), 3.99 (d, J = 11.7 Hz, 1H), 5.78 (dd, J = 9.3 Hz and J' = 2.9 Hz, 1H), 7.45 (t, J = 6.8 Hz, 1H), 7.56 (d, J = 6.8 Hz, 1H), 7.89 (d, J = 7.8 Hz, 1H), 8.21 (s, 1H). ^{13}C NMR ($CDCl_3$) δ: 22.1, 25.0, 29.3, 67.3, 85.9, 104.1, 115.5, 117.2, 124.7, 126.0, 127.1, 132.1, 139.2. LRMS/ESI: $[M+H]^+$ 228. LRMS/EI *m/z (%)*: 228 (16), 227 (M^+, 100), 199 (10), 168 (8), 156 (9), 144 (45), 143 (38). HRMS/EI *m/z* calcd for $C_{13}H_{13}N_3O$ $[M]^+$: 227.1059; found: 227.1053.

5.1.5.2. 1-(Tetrahydro-2*H*-pyran-2-yl)-1*H*-indazole-5-carbonitrile (8b). Starting from the 5-bromo-1-(tetrahydro-2*H*-pyran-2-yl)-1*H*-indazole **7b** (0.3 g, 1 mmol) and following the general procedure, the product **8b** was obtained as an orange solid (0.2 g, 79%). Mp 85 °C. TLC R_f = 0.31 (Silica gel; EtOAc/cyclohexane 1:3). IR (KBr): 2926, 2222, 1616, 1502, 1428, 1209, 1081, 1042, 994, 911, 808 cm^{-1}. ^1H NMR ($CDCl_3$) δ: 1.62-1.77 (m, 3H), 2.10-2.15 (m, 2H), 2.50-2.55 (m, 1H), 3.77 (t, J = 9.8 Hz, 1H), 4.02 (d, J = 11.7 Hz, 1H), 5.76 (dd, J = 9.3 Hz and J' = 2.9 Hz, 1H), 7.59 (d, J = 8.8 Hz, 1H), 7.71 (d, J = 8.8 Hz, 1H), 8.12 (s, 1H), 8.13 (s, 1H). ^{13}C NMR ($CDCl_3$) δ: 22.2, 25.0, 29.4, 67.4, 85.8, 104.8, 111.6, 119.5, 124.3, 127.4, 128.6, 134.5, 140.3. LRMS/ESI: $[M+H]^+$ 228. HRMS/EI *m/z* calcd for $C_{13}H_{13}N_3O$ $[M]^+$: 227.1059; found: 227.1057.

5.1.6. General procedure for the synthesis of 1*H*-indazole-4 and 5-carbonitriles (9a–b)

Indazole **8a** or **8b** was introduced in ethanolic HCl (5–15 mL) and the preparation was stirred for 3–6 h at room temperature. Then, the acidic mixture was neutralized thanks to a 2 N sodium hydroxide solution and ethanol was evaporated in vacuo. After addition of EtOAc (20 mL) to the residue, the organic layer was washed with brine (3 × 10 mL), dried over $MgSO_4$, filtered and evaporated in vacuo. Finally, the expected unprotected indazole-carbonitriles **9a–b** were in this case directly isolated.

5.1.6.1. 1*H*-Indazole-4-carbonitrile (9a). Starting from the 1-(tetrahydro-2*H*-pyran-2-yl)-1*H*-indazole-4-carbonitrile **8a** (0.1 g, 0.5 mmol) and following the general procedure, the product **9a** was obtained as a pinkish solid (0.06 g, 76%). Mp 132 °C. TLC R_f = 0.26 (Silica gel; EtOAc/cyclohexane 1:2). IR (KBr): 3434, 3165, 2925, 2854, 2228, 1615, 1370, 1266, 1089, 1031, 949, 784, 756 cm^{-1}. ^1H NMR (DMSO-d_6) δ: 7.51 (t, J = 6.8 Hz, 1H), 7.83 (d, J = 6.8 Hz, 1H), 7.94 (d, J = 8.8 Hz, 1H), 8.39 (s, 1H), 13.72 (s, 1H). ^{13}C NMR (DMSO-d_6) δ: 102.1, 116.1, 117.5, 122.2, 126.0, 127.0, 131.7, 139.6. LRMS/ESI: $[M+H]^+$ 144. Anal. calcd for $C_8H_5N_3$ (%): C, 67.13; H, 3.52; N, 29.35; found: C, 67.51; H, 3.50; N, 29.24.

*5.1.6.2. 1H-Indazole-5-carbonitrile (**9b**).* Starting from the 1-(tetrahydro-2*H*-pyran-2-yl)-1*H*-indazole-5-carbonitrile **8b** (0.1 g, 0.4 mmol) and following the general procedure, the product **9b** was obtained as a beige solid (0.05 g, 79%). Mp 177 °C. TLC R_f = 0.18 (Silica gel; EtOAc/cyclohexane 1:2). IR (KBr): 3435, 3132, 2954, 2873, 2221, 1625, 1292, 1076, 951, 911, 801 cm^{-1}. ^1H NMR (DMSO-d_6) δ: 7.70 (d, J = 8.8 Hz, 1H), 7.76 (d, J = 8.8 Hz, 1H), 8.31 (s, 1H), 8.44 (s, 1H), 13.62 (s, 1H). ^{13}C NMR (DMSO-d_6) δ: 102.7, 111.8, 119.9, 122.4, 127.7, 128.0, 134.8, 140.8. LRMS/ESI: $[M+H]^+$ 144. HRMS/EI *m/z* calcd for $C_8H_5N_3$ $[M]^+$: 143.0483; found: 143.0484.

5.2. In vitro biological evaluation

Effects of the different previously synthetized indazole derivatives on nNOS activity were evaluated in vitro on rat cerebellum homogenates. IC_{50} were determined from the NOS inhibition curves constructed with five concentrations (0.01, 0.1, 1, 10 and 100 μM). Enzymatic activities were assayed by monitoring the conversion of L-[3H]arginine to L-[3H]citrulline according to a previously described method (1 mM $CaCl_2$, 200 μM β-NADPH, 0.88 μM L-arginine, 0.12 μM L-[3H]arginine, 15 min at 37 °C).[34,36,47] nNOS basal activity represented 120 ± 15 pmol citrulline formed/mg protein/h and the already described lead compound, 7-NI (dissolved in DMSO 0.4%), exhibited an IC_{50} value of 0.6 ± 0.2 μM (mean ± SEM; n = 5 experiments).

5.3. Molecular modeling

For each docked compound a preliminary calculation on its protonation state at pH 7.4 was carried out using standard tools of the ChemAxon Package (http://www.chemaxon.com/) and the majority microspecie (corresponding to among 94–100% for different compounds) at this pH was used for docking studies.

The crystallographic coordinates of rat nNOSox used for docking studies were obtained from X-ray structure of the 3-bromo-7-NI/nNOSox complex (PDB ID 1OM5, a structure refined to 2.3 Å with an R factor of 23.1%).

Docking of compounds into nNOSox was carried out with the GOLD program (v 5.0) using the default parameters.[40] This program applies a genetic algorithm to explore conformational spaces and ligand binding modes. To evaluate the proposed ligand poses the ChemScore fitness function was applied in the docking studies. The binding site in the nNOSox was defined as a 10 Å sphere centered on the heme iron atom.

Molecular mechanics calculations on the nNOSox/indazole derivative complexes were performed using CHARMM program with potential function parameter set 22.[48] The Discovery Studio program was used to derive CHARMM force field parameters for the indazole derivatives applying MMFF partial charges.[49] During all calculations all atoms that lay 8 Å or further from any indazole derivative atoms were fixed.

For all energy minimizations, 500 steps of steepest descent, followed by 1000 steps of conjugate gradient and by n steps of Adopted Basis Newton-Raphson minimization were carried out until an average energy gradient, during a cycle of minimization, less than 10^{-3} kcal/(mol Å).

Acknowledgment

We thank Dr. Rémi Legay for the mass spectrometry measurements. We thank the CRIHAN (Centre de Ressources Informatiques de Haute-Normandie) and the European Community (FEDER) for the molecular modelling softwares.

References and notes

1. Bryan, N. S.; Bian, K.; Murad, F. *Front Biosci.* **2009**, *14*, 1.
2. Salerno, L.; Sorrenti, V.; Di Giacomo, C.; Romeo, G.; Siracusa, M. A. *Curr. Pharm. Des.* **2002**, *8*, 177.
3. Arzumanian, V.; Stankevicius, E.; Laukeviciene, A.; Kevelaitis, E. *Medicina* **2003**, *39*, 535.
4. Alderton, W. K.; Cooper, C. E.; Knowles, R. G. *Biochem. J.* **2001**, *357*, 593.
5. Förstermann, U.; Münzel, T. *Circulation* **2006**, *113*, 1708.
6. Villanueva, C.; Giulivi, C. *Free Radical Biol. Med.* **2010**, *49*, 307.
7. Brüne, B. *Pharmacol. Res.* **2010**, *61*, 265.
8. Toda, N.; Ayajiki, K.; Okamura, T. *Pharmacol. Rev.* **2009**, *61*, 62.
9. Vincent, S. R. *Prog. Neurobiol.* **2010**, *90*, 246.
10. Schmidtko, A.; Tegeder, I.; Geisslinger, G. *Trends Neurosci.* **2009**, *32*, 339.
11. Xu, L.; Mabuchi, T.; Katano, T.; Matsumura, S.; Okuda-Ashitaka, E.; Sakimura, K.; Mishina, M.; Ito, S. *Nitric Oxide* **2007**, *17*, 18.
12. Freire, M. A. M.; Guimaraes, J. S.; Gomes-Leal, W.; Pereira, A. *Front. Neurosci.* **2009**, *3*, 175.
13. Overeem, K. A.; Ota, K. T.; Monsey, M. S.; Ploski, J. E.; Schafe, G. E. *Front. Behav. Neurosci.* **2010**, *4*, 1.
14. Cheng, B.-C.; Chang, C.-P.; Lin, M.-T.; Lee, C.-C. *Neuropharmacology* **2007**, *52*, 297.
15. Moro, M. A.; Cardenas, A.; Hurtado, O.; Leza, J. C.; Lizasoain, I. *Cell Calcium* **2004**, *36*, 265.
16. Martinez-Murillo, R.; Fernandez, A. P.; Serrano, J.; Rodrigo, J.; Salas, E.; Mourelle, M.; Martinez, A. *Neurosci. Lett.* **2007**, *415*, 149.
17. Singh, S.; Dikshit, M. *Brain Res. Rev.* **2007**, *54*, 233.
18. Chung, K. K. K.; David, K. K. *Nitric Oxide* **2010**, *22*, 290.
19. Fidana, I.; Yuksel, S.; Ymir, T.; Irkeç, C. Nur Aksakal *F. J. Neuroimmunol.* **2006**, *171*, 184.
20. Chandra, A.; Enkhbaatar, P.; Nakano, Y.; Traber, L. D.; Traber, D. L. *Clinics* **2006**, *61*, 71.
21. Seo, J.; Martasek, P.; Roman, L. J.; Silverman, R. B. *Bioorg. Med. Chem.* **2007**, *15*, 1928.
22. Erdal, E. P.; Martasek, P.; Roman, L. J.; Silverman, R. B. *Bioorg. Med. Chem.* **2007**, *15*, 6096.
23. Lee, K.-S.; Lee, D.-K.; Jeoung, D.; Lee, H.; Choe, J.; Ha, K.-S.; Wond, M.-H.; Kwon, Y.-G.; Kim, Y.-M. *Biochem. Biophys. Res. Commun.* **2012**, *418*, 49.
24. Litzinger, E. A.; Martasek, P.; Roman, L. J.; Silverman, R. B. *Bioorg. Med. Chem.* **2006**, *14*, 3185.
25. Maccallini, C.; Patruno, A.; Lannutti, F.; Ammazzalorso, A.; De Filippis, B.; Fantacuzzi, M.; Franceschelli, S.; Giampietro, L.; Masella, S.; Felaco, M.; Re, N.; Amoroso, R. *Bioorg. Med. Chem. Lett.* **2010**, *20*, 6495.
26. Claramunt, M. R.; Lopez, C.; Perez-Medina, C.; Perez-Torralba, M.; Elguero, J.; Escames, G.; Acuna-Castroviejo, D. *Bioorg. Med. Chem.* **2009**, *17*, 6180.
27. Cottyn, B.; Acher, F.; Ramassamy, B.; Alvey, L.; Lepoivre, M.; Frapart, Y.; Stuehr, D.; Mansuy, D.; Boucher, J.-L.; Vichard, D. *Bioorg. Med. Chem.* **2008**, *16*, 5962.
28. Jaroch, S.; Hölscher, P.; Rehwinkel, H.; Sülzle, D.; Burton, G.; Hillmann, M.; McDonald, F. M. *Bioorg. Med. Chem. Lett.* **2003**, *13*, 1981.
29. Xue, F.; Fang, J.; Lewis, W. W.; Martasek, P.; Roman, L. J.; Silverman, R. B. *Bioorg. Med. Chem. Lett.* **2010**, *20*, 554.
30. Maddaford, S.; Renton, P.; Speed, J.; Annedi, S. C.; Ramnauth, J.; Rakhit, S.; Andrews, J.; Mladenova, G.; Majuta, L.; Porreca, F. *Bioorg. Med. Chem. Lett.* **2011**, *21*, 5234.
31. Annedi, S. C.; Maddaford, S. P.; Ramnauth, J.; Renton, P.; Speed, J.; Rakhit, S.; Andrews, J.; Porreca, F. *Bioorg. Med. Chem. Lett.* **2012**, *22*, 1980.
32. Crestey, F.; Lohou, E.; Stiebing, S.; Collot, V.; Rault, S. *Synlett* **2009**, *4*, 615.
33. Lohou, E.; Collot, V.; Stiebing, S.; Rault, S. *Synthesis* **2011**, *16*, 2651.
34. Schumann, P.; Collot, V.; Hommet, Y.; Gsell, W.; Dauphin, F.; Sopkova, J.; MacKenzie, E.; Duval, D.; Boulouard, M.; Rault, S. *Bioorg. Med. Chem. Lett.* **2001**, *11*, 1153.
35. Collot, V.; Sopkova-de Oliveira Santos, J.; Schumann, P.; Colloc'h, N.; MacKenzie, E.; Rault, S. *J. Enz. Inh. Med. Chem.* **2003**, *18*, 195.
36. Boulouard, M.; Schumann-Bard, P.; Butt-Gueulle, S.; Lohou, E.; Stiebing, S.; Collot, V.; Rault, S. *Bioorg. Med. Chem. Lett.* **2007**, *17*, 3177.
37. Li, H.; Martasek, P.; Masters, B. S.; Poulos, T. L.; Raman C. S. To be published (PDB ID: 1OM5).
38. Rosenfeld, R. J.; Garcin, E. D.; Panda, K.; Andersson, G.; Aberg, A.; Wallace, A. V.; Morris, G. M.; Olson, A. J.; Stuehr, D. J.; Tainer, J. A.; Getzoff, E. D. *Biochemistry* **2002**, *41*, 13915.
39. Sopkova-de Oliveira Santos, J.; Collot, V.; Rault, S. *Acta Cryst. C* **2000**, *56*, 1503.
40. Jones, G.; Willett, P.; Glen, R. C.; Leach, A. R.; Taylor, R. *J. Mol. Biol.* **1997**, *267*, 727.
41. Bouissane, L.; El Kazzouli, S.; Leonce, S.; Pfeiffer, B.; Rakib, E. M.; Khouili, M.; Guillaumet, G. *Bioorg. Med. Chem. Lett.* **2006**, *14*, 1078.
42. Cheung, M.; Boloor, A.; Stafford, J. A. *J. Org. Chem.* **2003**, *68*, 4093.
43. Lu, Y.; Wang, Y.; Xu, Z.; Yan, X.; Luo, X.; Jiang, H.; Zhu, W. *J. Phys. Chem. B* **2009**, *113*, 12615.
44. Baumli, S.; Endicott, J. A.; Johnson, L. N. *Chem. Biol.* **2010**, *17*, 931.
45. Chobanian, H. R.; Fors, B. P.; Lin, L. S. *Tetrahedron Lett.* **2006**, *47*, 3303.
46. Sheldrick, G. M. *Acta Cryst.* **2008**, *A64*, 112.
47. Dwyer, M. A.; Bredt, D. S.; Snyder, S. H. *Biochem. Biophys. Res. Commun.* **1991**, *176*, 1136.
48. Brooks, B. R.; Bruccoleri, R. E.; Olafson, B. D.; Sates, D. J.; Swaninathan, S.; Karplus, M. *J. Comput. Chem.* **1983**, *4*, 187.
49. MacKerell, J. A. D.; Bashford, D.; Bellott, M.; Dunbrack, J. R. L.; Evanseck, J. D.; Field, M. J.; Fischer, S.; Gao, J.; Guo, H.; Ha, S.; Joseph-McCarthy, D.; Kuchnir, L.; Kuczera, K.; Lau, F. T. K.; Mattos, C.; Michnick, S.; Ngo, T.; Nguyen, D. T.; Prodhom, B.; Reiher, I. W. E.; Roux, B.; Schlenkrich, M.; Smith, J. C.; Stote, R.; Straub, J.; Watanabe, M.; Wiorkiewicz-Kuczera, J.; Yin, D.; Karplus, M. *J. Phys. Chem. B* **1988**, *102*, 3586.